Hum. Reprod. Advance Access published May 9, 2011
Human Reproduction, Vol.0, No.0 pp. 1–17, 2011
doi:10.1093/humrep/der140

human reproduction

ORIGINAL ARTICLE *Reproductive biology*

Evidence that carbonyl stress by methylglyoxal exposure induces DNA damage and spindle aberrations, affects mitochondrial integrity in mammalian oocytes and contributes to oocyte ageing

Carla Tatone[1†], Tanja Heizenrieder[2†], Giovanna Di Emidio[1], Patrick Treffon[2], Fernanda Amicarelli[3], Thorsten Seidel[4], and Ursula Eichenlaub-Ritter[2,*]

[1]Department of Health Sciences, University of L'Aquila, Via Vetoio, 67100 L'Aquila, Italy [2]Faculty of Biology, Gene Technology Microbiology, University of Bielefeld, 33501 Bielefeld, Germany [3]Department of Basic and Applied Biology, University of L'Aquila, Via Vetoio, 67100 L'Aquila, Italy [4]Faculty of Biology, Dynamic Cell Imaging, University of Bielefeld, 33501 Bielefeld, Germany

*Correspondence address. Tel: +49-(0)-521-106-4832/6907; Fax: +49-(0)521-106-6015; E-mail: eiri@uni-bielefeld.de

Submitted on October 28, 2010; resubmitted on March 2, 2011; accepted on March 30, 2011

BACKGROUND: Highly reactive carbonyl compounds formed during glycolysis, such as methylglyoxal (MG), can lead to the formation of 'advanced glycation end products' (AGE) and carbonyl stress. Toxic AGEs are suspected to accumulate and play a role in reducing quality and developmental potential of mammalian oocytes of aged females and in PCOS and diabetic patients. Whether and how MG and AGE affect young and aged oocytes at the cellular level is unknown.

METHODS: The study consists of three parts. In Part A expression of MG-detoxifying enzymes glyoxalases 1 and 2 was analysed by RT–PCR at different stages of maturation in denuded oocytes (DO), cumulus–enclosed oocytes (CEO) and metaphase (M)II oocytes of the CD-1 mouse to obtain information on stage-specific susceptibility to carbonyl stress. DO and CEO from young and aged females and from stimulated cycles were exposed to MG during maturation *in vitro* to assess also age-related changes in sensitivity to carbonyl stress induced by MG. Induction of apoptosis by MG on *in vitro* maturing DO was assessed by terminal deoxynucleotidyl transferase-mediated dUDP nick-end labelling test. In Part B of the study, DO from large antral follicles of ovaries of adult, young MF-1 mice in late diestrous were exposed to MG to assess direct influences of MG and AGEs formed during continuous exposure to MG on rate and kinetics of maturation to MII, on DNA integrity (by γ-H2AX staining) in the germinal vesicle (GV) stage, and on spindle formation and chromosome alignment (by tubulin and pericentrin immunofluorescence and polarization microscopy), and chromosome segregation (by C-banding) during *in vitro* maturation. Since MG and AGEs can affect functionality of mitochondria in Part C, mitochondrial distribution and membrane potential was studied using JC-1 probe. Expression of a redox-sensitive mito-Grx1-roGFP2 protein in mitochondria of maturing oocytes by confocal laser scanning microscopy was employed to determine the inner mitochondrial glutathion (GSH)/glutathion disulfide (GSSG)-dependent redox potential.

RESULTS: Part A revealed that mRNA for glyoxalases decreases during meiotic maturation. Importantly, cumulus from aged mice in CEO obtained from stimulated cycles does not protect oocytes efficiently from MG-induced meiotic arrest during *in vitro* maturation. Part B showed that the MG-induced meiotic delay or arrest is associated with significant rises in spindle aberrations, chromosome congression failure and aberrant telophase I in oocytes. MG exposure of meiotically arrested GV-stage oocytes significantly increases the numbers of γ-H2AX spots in the nucleus suggesting increased DNA damage, while MG exposure during maturation affects chromatin condensation and induces chromosome lagging at anaphase I. Moreover, Part C revealed that carbonyl stress by chronic exposure to MG is associated

[†] These authors contributed equally to the study.

with delays in changes in mitochondrial distribution and altered inner-mitochondrial GSH/GSSG redox potential, which might be particularly relevant for cytoskeletal dynamics as well as processes after fertilization. Sensitivity to a meiotic block by MG appears dependent on the genetic background.

CONCLUSIONS: The sensitivity to carbonyl stress by MG appears to increase with maternal age. Since MG-exposure induces DNA damage, meiotic delay, spindle aberrations, anaphase I lagging and epimutation, aged oocytes are particularly at risk for such disturbances in the absence of efficient protection by cumulus. Furthermore, disturbances in mitochondrial distribution and redox regulation may be especially critical for fertilization and developmental competence of oocytes exposed to MG and carbonyl stress before or during maturation, for instance, in aged females, or in PCOS or diabetic patients, in agreement with recent suggestions of correlations between poor follicular and embryonic development, lower pregnancy rate and presence of toxic AGEs in serum, irrespective of age.

Key words: oocyte quality / ageing / advanced glycation end product / spindle / mitochondria

Introduction

Ovarian functional decline with age entails a gradual depletion of ovarian follicle reserve and a reduced ability to produce oocytes competent for fertilization and embryo development (Tatone *et al.*, 2008; Broekmans *et al.*, 2009). Ovarian physiology is unique in that follicles might remain in a 'resting' phase for a long time and start growing even in the fifth decade of life. Based on this concept, it is reasonable to hypothesize that during the reproductive lifespan, the ovarian microenvironment is gradually perturbed. Ovarian ageing is associated with the impairment of specific functions of oocytes and granulosa cells, along with general dysfunctions typical of the cellular ageing process, such as altered mitochondrial activity, energetic failure and changes in genes and protein expression profiles (Van Blerkom *et al.*, 1998; Eichenlaub-Ritter *et al.*, 2004; Hamatani *et al.*, 2004; Thouas *et al.*, 2005; Steuerwald *et al.*, 2007; Grondahl *et al.*, 2010). A relevant consequence of this condition is an increased susceptibility to meiotic errors enhancing the risk of chromosomal abnormalities in the mature oocyte (Eichenlaub-Ritter, 1998; Vogt *et al.*, 2008; Hassold and Hunt, 2009). In addition, embryo development in advanced reproductive age may be jeopardized by altered epigenetic mechanisms (Lopes *et al.*, 2009).

It has been proposed that ovarian follicles become exposed to factors that irreversibly accumulate during the reproductive lifespan (Tatone *et al.*, 2008) that act synergistic to suboptimal follicular environment on maturation, chromosomal constitution and developmental capacity of the oocyte (Eichenlaub-Ritter, 2003). Accumulation of spontaneous damage during normal metabolism plays a relevant role in the cellular ageing process (Yin and Chen, 2005; Rattan, 2008). Biological reactions leading to ageing include modifications of different kinds of molecules by free radicals and glycation (Yin *et al.*, 2001; Harman, 2006). The latter is a non-enzymatic reaction by which highly reactive carbonyl compounds formed during glycolysis and other metabolic pathways react with biomolecules leading to the formation of AGEs (advanced glycation end products), the most relevant hallmarks of ageing. By adversely affecting structural and functional properties of proteins, lipids and DNA (Ledl and Schleicher, 1999; Baynes, 2001; Yin *et al.*, 2001), glycation causes tissue damage resulting from molecular cross-linking (Verzijl *et al.*, 2000) and changes in gene expression through AGE receptor (Schmidt *et al.*, 2000; Wautier *et al.*, 2001). Reactive carbonyl compounds overload, a condition known as carbonyl stress, can be caused by decreased detoxification or increased formation via oxidative stress. A major precursor of AGEs is the α-oxoaldehyde methylglyoxal (MG), a dicarbonyl compound, which is physiologically produced during the glycolytic process and other physiological pathways and which can inhibit mitochondrial respiration and proliferation, induce apoptosis and increase reactive oxygen species (ROS) production (Thornalley, 1996; Amicarelli *et al.*, 2003). Detoxification of MG mainly occurs via the glyoxalase system, which consists of two enzymes: glyoxalase I (GLO1) and hydroxyacyl glutathione hydrolase (HAGH, previously known as glyoxalase 2, GLO2). GLO1 catalyses the formation of *S*-D-lactoylglutathione from MG with reduced glutathione (GSH) acting as a cofactor. HAGH catalyses the hydrolysis of *S*-D-lactoyl-glutathione to D-lactate and regenerates GSH (Mannervik, 2008). The glyoxalase system, particularly GLO1, represents the frontline defence against dicarbonyl glycation in physiological systems (Thornalley, 2003; Kuhla *et al.*, 2006), limiting carbonyl stress toxicity (Shinohara *et al.*, 1998). Knockdown of GLO1 decreases lifespan while overexpression may prolong life (Morcos *et al.*, 2008). AGEs may be involved in ovarian physiopathology, e.g. in PCOS patients (Diamanti-Kandarakis *et al.*, 2007). Furthermore, MG may be involved in reduced developmental competence of oocytes and embryos from diabetic patients (Chang and Chan, 2010). A role for AGEs in ovarian ageing has also been suggested by some observations in human follicular fluids (Fujii and Nakayama, 2010). In the CD-1 mouse model, a recent study revealed an age-related increase in MG and AGEs in relation to decreased expression of GLO1 and relevant damage to the ovarian proteome (Tatone *et al.*, 2010).

In Part A of this investigation, we therefore addressed the question whether mouse oocytes are equipped with a defence system against reactive carbonyl compounds by monitoring the expression of *Glo1* and *Glo2* genes in germinal vesicle (GV) and *in vivo* matured and ovulated metaphase II (MII) oocytes from the CD-1 strain. We found that both genes were expressed at GV stage but undetectable in MII oocytes such that the mature female gamete may be particularly vulnerable to carbonyl stress. Furthermore, we investigated potential deleterious effects of carbonyl stress produced by chronic exposure to MG by exposing DO and cumulus-enclosed oocytes (CEO) from pregnant mare serum (PMSG)-stimulated adult outbred CD-1 mice to this compound during *in vitro* maturation. This revealed that protection to adverse effects by MG mediated by cumulus decreases with age.

The Part B of the study was devoted to analyse the direct influences of chronic MG and carbonly stress on *in vitro* maturing, unprotected oocytes that were denuded from cumulus and originated from

unstimulated MF-1 mice (Roberts *et al*., 2005), yielding large numbers of maturation-competent oocytes in order to assess spindle formation and chromosome behaviour. While genotoxic agents that induce DNA damage may be cytotoxic and induce degeneration of GV-stage oocytes (Bradshaw *et al*., 1995) exposures that are not cytotoxic and cause spindle aberrations that may induce a delay or block in maturation after GVBD, when the spindle assembly checkpoint (SAC) is not satisfied and chromosomes do not become stably attached to spindle fibres (reviewed by Vogt *et al*., 2007; Holt and Jones, 2009). We therefore evaluated the effects of different MG concentrations on meiotic progression after 16 and 19 h of incubation and the impact on spindle integrity and chromosomal constitution. To mimic the situation in an aged ovary, in which defences by detoxification are already declined, we also studied the potential DNA-damaging influences of carbonyl stress by chronic MG exposure of GV-stage oocytes blocked from spontaneous resumption of maturation by culture in the presence of cilostamide, a specific phosphodiesterase 3 inhibitor (Nogueira *et al*., 2005). Numbers of γ-H2AX-antibody reactive foci were subsequently analysed in the nucleus as markers of DNA lesions and repair (e.g. Rogakou *et al*., 1998; Tanaka *et al*., 2006; Mah *et al*., 2010).

In Part C of the study, we analysed the influences of MG exposure on mitochondrial distribution and potential of the inner-mitochondrial membrane ($\Delta\Psi_{mit}$; Van Blerkom *et al*., 2002) and the intramitochondrial GSH/GSSH redox state (E^{m}_{GSH}; Meyer and Dick, 2010) since mitochondrial dysfunction can be at the basis of spindle and chromatin alterations and reduced developmental potential. Although oocytes have little glycolysis, the presence of mitochondria in the vicinity of the spindle may be important for local ATP supply at maturation, and a cortical domain rich in functionally intact mitochondria with high $\Delta\Psi_{mit}$ appears essential for calcium signalling and repetitive membrane depolarization at fertilization (Van Blerkom *et al*., 2002, 2008; Van Blerkom, 2009). Since GSH protects oocytes, the zygote and embryo from oxidative damage and alterations in GSH/GSSG ratio compromise developmental potential (e.g. Curnov *et al*., 2010), we assessed the intramitochondrial GSH-depedent redox potential in controls and MG-exposed oocytes using a novel non-invasive approach.

Materials and Methods

Part A. Expression of Glo1 and Glo2 and age-related sensitivity to MG

Animals and oocyte collection

Outbred CD-1 mice (Charles River Italia s.r.l., Calco, Italy) at the age of 4–8 weeks (young mice) and 48–52 weeks (reproductively aged mice) were used to obtain CEO or denuded oocytes (DO) from stimulated females or from unprimed mice (Tatone *et al*., 2006). The mice were superovulated by intraperitoneal injection of 10 IU of PMSG (Folligon; Intervet-International, Boxmeer, Holland) and 10 IU of hCG (Profasi HP 2000; Serono, Roma, Italy) 48 h apart (for study flow chart, see Fig. 1). For expression studies, oocytes arrested at MII stage were released at 15 h post-hCG from the oviducts into M2 medium (Sigma, St. Louis, MO). Cumulus was removed by brief exposure to 0.3 mg/ml hyaluronidase (Sigma).

Analysis of Glo1 and Glo2 expression by semi-quantitative RT–PCR

Denuded GV-stage oocytes from unprimed mice or whole CEO with oocytes and cumulus cells or MII oocytes from stimulated cycles were washed in phosphate-buffered saline (PBS) containing 3 mg/ml polyvinylpyrrolidone (PBS-PVP), transferred into a 0.6 ml tube in a volume <2 μl and immediately subjected to thermolysis and reverse transcription by cell-to-cDNA kit (Ambion, Inc., Austin, TX). Fifty microlitres containing the cDNA equivalent of 15 oocytes and PCR buffer 1X (Perkin Elmer Life And Analytical Sciences, Boston, MA), 1.5 mM $MgCl_2$, 0.2 mM of each dNTP, 0.2 mM of each primer and 1.25 U of Taq polymerase (all products from Perkin Elmer) were used in PCR in duplicate and in multiplex reactions, using 18S as the internal standard (QuantumRNA Classic 18S; Ambion), producing a 489-bp PCR product. The 18S rRNA internal control is used in combination with 18S competimers and a gene-specific PCR primer pair. The correct ratio between the 18S rRNA primers and 18S competimers was empirically determined. Primers sequences for *Glo1* were derived from GeneBank (gi|31981281|ref|NM_025374.2| *Mus musculus* GLO1, *Glo1*, mRNA), with primer pair: forward, GATTTGGTCA CATTGGGATTGC; reverse, TCCTTTCATTTTCCCGTCATCAG and amplification product of 110 bp. The primer sequences of *Glo2* provided by GeneBank (gi|227499237|ref|NM_024284.2| *Mus musculus* GLO2 (HAGH), *Glo2*, mRNA) were: 5′ GATGAGGACACCCAGGAGG and 3′ ACAGCCAGCAACAAACAAT, producing a 369 bp amplification product. The number of cycles was between 22 and 40 cycles according to approximate midpoint of the linear amplifications (35 cycles). PCR thermal cycling for *Glo1* and *Glo2* mRNA amplification and classic 18S was 95°C for 5 min for 1 cycle; 94°C for 40 s, 59°C for 1 min, 72°C for 2 min for 35 cycles; 72°C for 5 min. PCR products were electrophoresed (10 V/cm) in 1.5% ethidium bromide stained-agarose gel in 44.5 mM Tris, 44.5 mM borate, 1 mM EDTA (TBE) buffer. The relative intensities of transcript-specific PCR products, normalized to those obtained from 18S amplification, were determined by NIH image software. Values were given as relative units. Experiments were performed in triplicate.

Exposure of DO and CEO from CD-1 mice to MG

DO and CEO were isolated from the ovaries of young and aged PMSG-primed mice 48 h after PMSG (Fig. 1), placed into M16 medium (Sigma, St. Luis, MO) in the presence or absence of MG (Sigma) (75–500 μM), and matured for 19 h in a humidified incubator at 37°C and 5% CO_2. Numbers of oocytes that resumed maturation and emitted the first polar body were recorded.

Analysis of MG-induced apoptosis

In vitro matured DO of controls and MG-exposed group (300 μM MG; 19 h) of young CD-1 mice were exposed to Tyrode's solution for 1 min in order to remove the zona pellucida and permeabilized for 5 min in 0.1% TritonX-100 in PBS-PVP. DNA fragmentation was detected by terminal deoxynucleotidyl transferase-mediated dUDP nick-end labelling (TUNEL) method by means of '*in situ*'; Cell Death kit (Roche Diagnostic Gmbh, Mannheim, Germany; 37°C for 1 h in 25 μl of 'TUNEL reaction mixture' containing dUTP-FITC, terminal deoxynucleotydil transferase enzyme and reaction buffer). Positive control was represented by oocytes treated with 50 U/ml DNase. Negative control was without dUTP-transferase enzyme. After washing in PBS-PVP, the oocytes were incubated in Hoechst 33342 (Sigma) at room temperature, mounted on slides and observed by epifluorescence microscope at ×400 magnification with appropriate filters.

Part B and C. Direct influences of MG on resting or *in vitro* maturing mouse oocytes

Animals, oocyte collection and maturation in vitro

For these experiments, outbred MF-1 mice were used which contain large numbers of large antral follicles at late diestrous of the natural cycle in the ovaries of young adult females. Maturation competent oocytes contain a

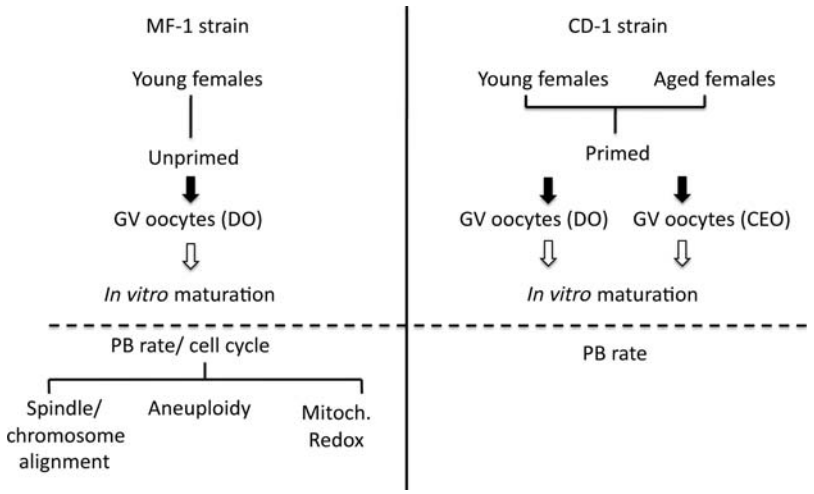

Figure 1 Flow chart of the experimental design for testing MG effects and age on *in vitro* maturation to metaphase II, and spindle, chromosomes and mitochondria employing the MF-1 and CD-1 strain of mice.

clear cytoplasm with little pigmentation that are ideally suited for spindle immunofluorecence (e.g. Eichenlaub-Ritter and Betzendahl, 1995; Vogt *et al.*, 2010). Outbred MF-1 mice were maintained in a temperature controlled environment under a 12 h light/dark cycle (7.00–19.00) at the Bielefeld University animal house with feed (R/M pellets; Sniff, Soest, Germany) and water *ad libitum*. All experiments were done under permit of the University authorities and in accordance with German law. Vaginal smears were used to obtain oocytes in late diestrous from large antral follicles of adult 2–4 months old MF-1 mice (Vogt *et al.*, 2009).

Cumulus-denuded oocytes were placed into M2 medium (Quinn *et al.*, 1982; all components obtained from Sigma, Deisenhofen, Germany), with or without MG (Sigma) and matured for 16 or 19 h in a humidified incubator at 37°C (Fig. 1).

Part B

Analysis of DNA damage by MG by staining with γ-H2AX

GV-stage oocytes from large antral follicles of MF-1 females in diestrous were placed into M2 medium, cultured for 5 h in the presence of 10 μM cilostamide (Sigma) without or with 75-μM MG, fixed for immunofluorescence (after removal of the zona by pronase followed by extraction in a microtubule-stabilizing solution containing Triton-X-100; Vogt *et al.*, 2009), and finally labelled by first antibody, anti-γ-H2AX antibody (Abcam, London, UK), followed by second anti-mouse-FITC-coupled antibody (Sigma) and staining of chromatin by 2-diamidino-2-phenylindole (DAPI, Sigma; 10 μg/ml in PBS). Oocytes were viewed by Zeiss Axiophot fluorescence microscope (Zeiss, Jena, Germany) with 100× objective lens. Images of an optical section were taken through the centre of the nucleus at its largest diameter (Trapphoff *et al.*, 2010) to count numbers of γ-H2AX spots in controls and MG-exposed GV oocytes.

Spindle and pericentrin immunofluorescence with oocytes from MF-1 mice

Oocytes were processed for tubulin-immunofluorescence as previously described (Eichenlaub-Ritter and Betzendahl, 1995; Sun *et al.*, 2004). Immunolabelling was subsequently with first antibody [e.g. rabbit anti-pericentrin-antibody (Covance, Munich, Germany) and/or mouse anti-tubulin (Sigma)] and second antibody [anti-rabbit-TRITC (Sigma) and/or anti-mouse-FITC (Sigma)] followed by staining of chromatin by DAPI (Sigma) or propidium-iodide (Sigma) and mounting in PBS with 20 μl/ml diamino-bicyclo-octane. Images were viewed by Zeiss Axiophot fluorescence microscope and recorded by Axiovision system (Zeiss) or confocal microscope (Leica TCS SP2; Leica Microsystems, Germany). Morphology of spindle and alignment of chromosomes as well as pericentrin at spindle poles was analysed in controls and MG-exposed group.

Octax polarization microscopy: non-invasive analysis of meiotic delay in MG-exposed oocytes

Meiotic progression to GV breakdown (GVBD) or emission of the first polar body (PB) was analysed by Octax Eye-Ware polarization microscope (OCTAX EyeWare MX, MTG. Altendorf, Germany) equipped with a heated stage on a Nikon microscope with 20× objective lens and appropriate filters and LCD liquid crystal optics and hardware for imaging and recording for qualitative and quantitative polarization microscopy (Shen *et al.*, 2008; Vogt *et al.*, 2009; Trapphoff *et al.*, 2010). Oocytes in a microdrop of 10 μl M2 medium covered with warm mineral oil (Sigma) matured in a WilCO Wells BV dish with glass bottom (GWSt-5040, Amsterdam, Netherlands). Images were taken at 2 min intervals to assess nuclear membrane breakdown (GVBD) and anaphase I progression and first polar body formation (Vogt *et al.*, 2009, 2010).

Chromosomal analysis

Spreading after hypotonic treatment, C-banding and chromosome analysis of oocytes were carried out as previously described (Eichenlaub-Ritter and Boll, 1989; Cukurcam *et al.*, 2003; Cukurcam *et al.*, 2007).

Part C

Analysis of mitochondrial distribution by JC-1 staining

Live staining of mitochondria was performed after incubating oocytes at different stages of maturation (7, 8 h or 16 h) for 30 min in warm M2 medium containing 1.5 μM JC-1 (5,5′,6,6′tetrachloro-1,1′,3,3′-tetrae-thyl-benzimidazolylcarbocyanin jodid; Molecular Probes). Lipophilic JC-1 accumulates within mitochondria and in its polarized state produces a green fluorescence which shifts to orange/red emission in case of more depolarized membrane potential (Van Blerkom *et al.*, 2002). JC-1-stained oocytes were viewed and recorded by fluorescence microscope (Zeiss). Numbers of oocytes with prominent accumulation of mitochondria with low potential of the inner-mitochondrial membrane (low ψ_{mit}) around

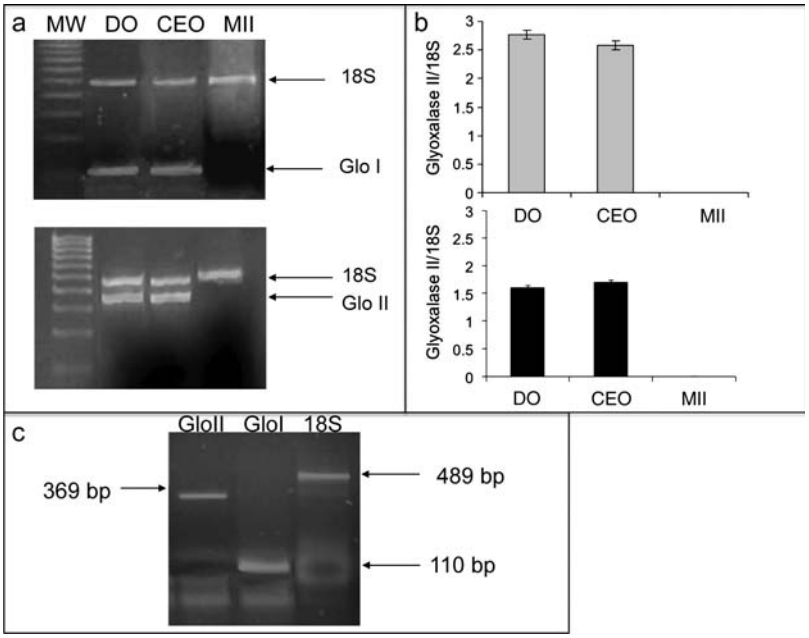

Figure 2 Expression of GLO1 and GLO2 in GV oocytes from unprimed mice, whole CEO from primed females and *in vivo* matured and ovulated MII oocytes (MII) from stimulated cycles (**a**,**b**) and cumulus cells from CD-1 mouse (**c**). *Glo1* and *Glo2* mRNA levels were analyzed in DO, CEO and MII oocytes by means of semi-quantitative RT–PCR (**b**). The assays were performed three times and shown are representative experiments (**a**) and the results of densitometric analysis test normalized to the corresponding value of the internal housekeeping gene (18S) (**b**). Data represent means ± SEM; *Glo1*, DO versus CEO, $P > 0.05$; *Glo2*, DO versus CEO, $P > 0.05$; *Glo1* DO versus *Glo2* DO, $P < 0.05$ (a,b); *Glo1* and *Glo2* mRNA levels were analyzed in cumulus cells by means of semi-quantitative RT–PCR in cumulus obtained from denuding CEO (**c**). The assays were performed two times and shown is a representative experiment.

the spindle (category: ++), those with more dispersed distribution throughout the ooplasm (category: +−) and those without visible accumulation in the proximity of spindle and chromosomes (category: −−) as well as number of oocytes with mitochondria with high ψ_{mit} in the periphery of the oocyte, close to the oolemma (category: ++) and such without mitochondrial accumulation at the oolemma (category: −−) were recorded.

Non-invasive analysis of the inner-mitochondrial GSH redox potential

We used a construct encoding for a fungal mitochondrial signal sequence, the human glutaredoxin-1 (*Grx1*), an enzyme that interacts specifically with the GSH/GSSG system (Gutscher *et al.*, 2008), and a redox-sensitive roGFP2 for specific live imaging of the inner-mitochondrial redox potential (E^{m}_{GSH}) (Meyer and Dick, 2010). The cDNA of Mito-Grx1-roGFP2 was amplified from pLCPX-Mito-Grx1-roGFP2 (kindly supplied by Andreas Meyer) using the following primer pairs: TCA GAT CTA GAG ATG GCC TCC ACT CGT G; TAT TTT CTA GAT TTA CTT GTA CAG CTC GTC CAG C and cloned into a pspO-vector. This construct was used for *in vitro* transcription followed by *in vitro* polyadenylation of the resultant RNA (Vogt *et al.*, 2009; Eichenlaub-Ritter *et al.*, 2010a,b). Polyadenylated mRNA was microinjected into denuded GV oocytes arrested in dicytate stage in M2 medium containing 0.5 μM cilostamide using an injector (model 5242, Eppendorf Hamburg/Germany), an automatic micromanipulator (model 5171, Eppendorf, Hamburg, Germany) and an inverse microscope (Axiovert 35, Zeiss, Jena, Germany). After 8 h for translation of mRNA into protein, DO were matured *in vitro* for 16 h in M2 medium without (control) or with 100 μM MG in the absence of cilostamide.

E^{m}_{GSH} was analysed in three independent experiments in MII oocytes expressing the fusion protein in mitochondria accumulated in the vicinity of the spindle (control: $n = 32$; MG: $n = 21$) by confocal laser scanning microscope (Leica TCS SP2; Leica Microsystems) with sequential excitation of Mito-Grx1-roGFP2 at 405 and 488 nm. Emission was recorded in the range of 500–530 nm in the area of the ooplasm in proximity of the spindle. Cells fully oxidized or reduced by exposure to 10 mM H_2O_2 and 10 mM DTT, respectively, served as standard.

According to Nernst equation, the redox potential was determined using the following equations:

(1) Calculation of oxidized degree of roGFP2

$$OxD_{roGFP2} = \frac{R - R_{red}}{I_{488ox}/I_{488red}(R_{ox} - R) + (R - R_{red})}$$

where R is the ratio of emission intensities (I) after excitation at 405 or 488 nm ($R = I_{405nm}/I_{488nm}$). For the determination of R_{ox} and R_{red} as well as I_{488ox} and I_{488red}, the mean values obtained from the *in situ* calibration, after complete oxidation and reduction by treatment with 10 mM DTT or H_2O_2, respectively, were used.

(2) pH correction

Because the midpoint potential of roGFP2 was determined at pH 7, a pH correction is required (Schafer and Buettner, 2001; Hanson *et al.*, 2004;

Gutscher et al., 2008). We assumed a pH value of 7.98 for mitochondria (Llopis et al., 1998).
(3)

$$E'_0\mathrm{pH} = E'_0 - 60.1\ \mathrm{mV} \times (\mathrm{pH} - 7)$$

Estimation of redox potential according to Nernst equation

$$E' = E'_{0(\mathrm{roGFP2})}\mathrm{pH} - \frac{2.303RT}{zF}\log_{10}\frac{1 - \mathrm{OxD_{roGFP2}}}{\mathrm{OxD_{roGFP2}}}$$

R is the universal gas constant ($R = 8.315\ \mathrm{JK^{-1}\ mol^{-1}}$), T the absolute temperature [$T = 310.5$ K (=37°C)], z the number of transferred electrons ($z = 2$) and F the faraday constant ($F = 96\,480\ \mathrm{C\ mol^{-1}}$). For $\mathrm{OxD_{roGFP2}}$, the cell-specific data, obtained from (1), were inserted.

Statistical analysis

For each experimental series, values are reported as mean ± SEM except for E^{m}_{GSH} for which mean and standard errors are shown. Statistical analysis was by Student t-test or chi-square test and SigmaStat software (Jandel Scientific Corporation, San Rafael, CA). For small numbers, chi-square with Yates correction was used. A P value of <0.05 was considered statistically significant.

Results

Part A: Expression of Glo1 and Glo2 and age-related sensitivity of oocytes to MG

Expression of GLO1 and 2 in oocytes and cumulus cells

Since glyoxalases were detected in whole mouse ovaries (Tatone et al., 2010), we now monitored GLO1 and GLO2 expression by semi-quantitative RT–PCR. Both *Glo1* and *Glo2* mRNAs were identified in GV-stage oocytes from DO of unstimulated cycles and whole cumulus–oocyte complexes (CEO groups) after PMSG stimulation, whereas they appeared undetectable in *in vivo* matured and ovulated MII oocytes from stimulated cycles (Fig. 2a and b). The two transcripts were also found in cumulus cells (Fig. 2c) with a pattern of expression similar to that observed in CEO (Fig. 2a).

MG effects on in vitro *maturation of young and reproductively aged mice*

In order to investigate whether the reproductive ageing affects oocyte susceptibility to MG toxicity, DO and CEO from young and reproductively aged PMSG-stimulated CD-1 mice (Fig. 1) were exposed to different MG concentrations in M16 medium and monitored for polar body formation after 19 h. Polar body emission was inhibited by MG in a dose-dependent manner in both the CEO and DO groups in the oocytes from young CD-1 mice, with a minimum effective dose of 150 μM (Fig. 3a). Nevertheless, DO oocytes exposed to 150 and 300 μM MG exhibited a percentage of polar body emission significantly lower than that observed in CEO ($P < 0.001$). When DO and CEO oocytes from reproductively old mice were subjected to the same MG treatments as young mice, CEO underwent maturation to a similar extent as DO oocytes in all groups (Fig. 3b).

Comparison of polar body emission of old and young groups revealed that values in old DO did not significantly differ from those observed in young DO at all concentrations tested whereas CEO from reproductively old mice were more sensitive to MG than CEO from the young group (Fig. 3).

Forty-three per cent of the 81 young oocytes exposed to 300-μM MG displayed TUNEL-positive DNA after 19 h of maturation and all of them showed condensed chromatin as characteristic for apoptosis (Fig. 4d,d′).

Part B: Disturbances by chronic MG exposure on resting and *in vitro* maturing mouse oocytes

Oocyte degeneration, meiotic arrest and meiotic delay

To test mutagenic or aneugenic effects of MG, we exposed denuded mouse oocytes of the MF-1 outbred strain to different concentrations of MG during 16 and 19 h of culture. Very few oocytes of the control from unprimed MF-1 females degenerated, whereas the majority matured to MII and emitted a first polar body during

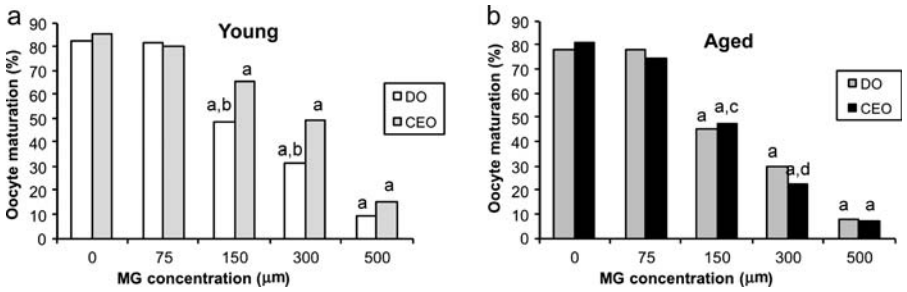

Figure 3 Effects of MG on *in vitro* maturation of oocytes from young (**a**) and reproductively aged (**b**) PMSG-stimulated CD-1 mice matured *in vitro* in M16 medium in the presence of different MG concentrations and monitored for polar body formation after a 19 h-incubation period. Values are expressed as percentages of total oocytes at each data point investigated. Chi-square analysis: significant difference between treated and controls (a: $P < 0.01$), between DO and CEO (b: $P < 0.001$), and between young and aged CEO (c: $P = 0.026$; d: $P < 0.001$). For further explanation, see text.

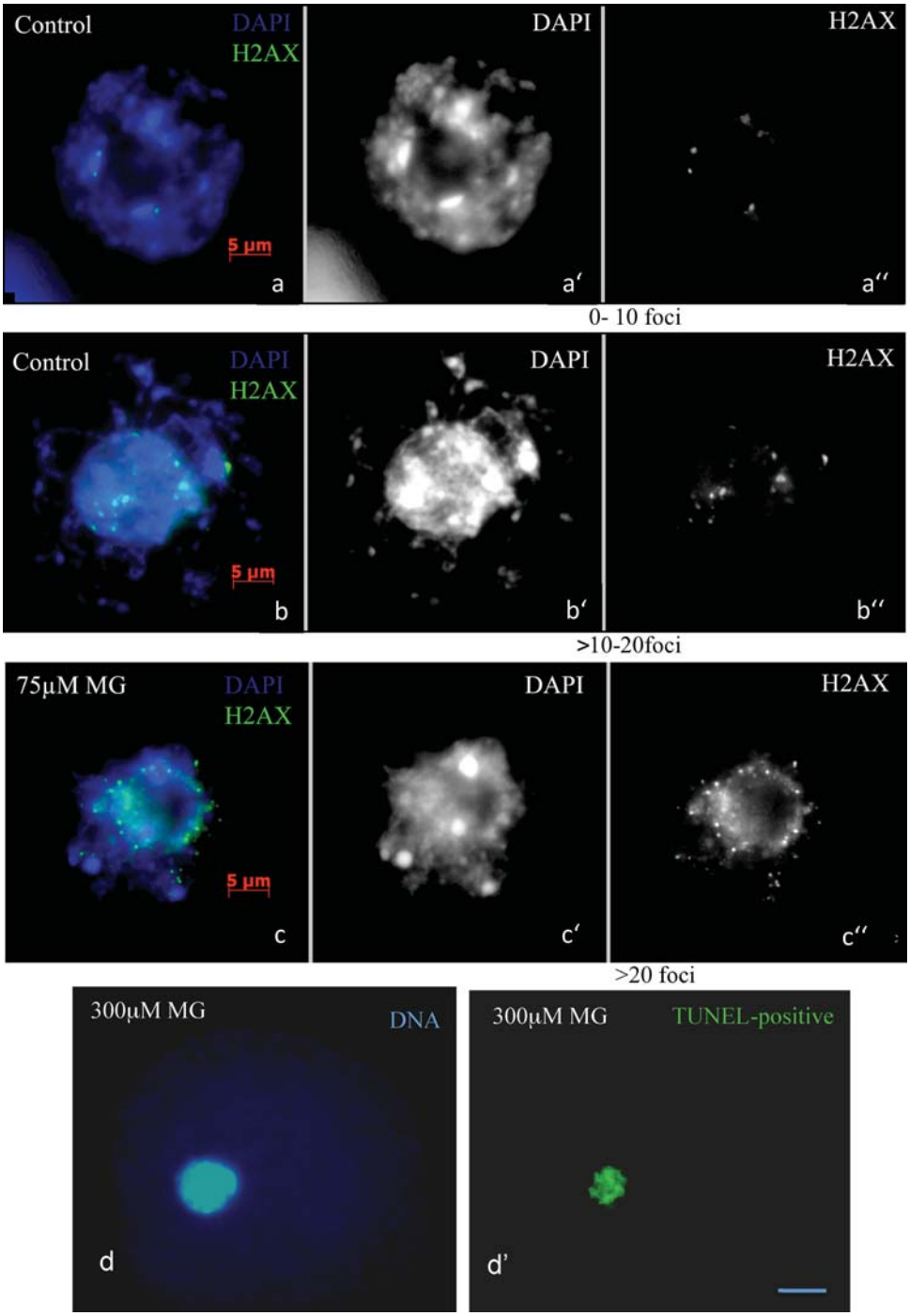

Figure 4 Induction of γ-H2AX foci in MG-exposed GV-stage oocytes of MF-1 mice (**a**–**c**″) and activation of an apoptotic pathway by MG in oocytes of CD-1 mice (**d,d**′). Representative samples of control GV-stage arrested oocytes with γ-H2AX 0–10 foci (**a**–**a**″) and with γ-H2AX >10–20 foci (**b**–**b**″) and oocytes exposed to 75-µM MG for 5 h during GV-stage arrest by cilostamide with >20 γ-H2AX foci (**c**–**c**″). (**a**–**c**) Double staining of chromatin for DNA (DAPI, blue) and γ-H2AX foci (fluorescein-coupled antibody, green) and DAPI and γ-H2AX foci alone (**a**′–**c**′**, a**″**b**″, respectively.); bars (red) for **a**–**c**″: 5 µm. (**d**–**d**′) Micrographs of a representative oocyte of CD-1 mouse exposed to 300-µM MG for 16 h and positively stained for DNA fragmentation using the TUNEL method. (d′) Blue fluorescence (Hoechst 33342), indicating DNA; (d)' Greenish-blue fluorescence (fluorescein), indicating fragmented DNA. Bar in **d**″ = 10 µm.

16 h of maturation *in vitro* (Control, 16 h, Table I). Concentrations of MG ≥150 µM caused already oocyte degeneration (Table I). Since no or only few oocytes matured with 300-µM MG group or developed to MII in the 150-µM MG group, respectively (Table I) we did not pursue further experiments with these higher concentrations of MG.

Table I Degeneration, GV-stage meiotic arrest or progression to GVBD or PB emission of denuded oocytes of MF1 mice cultured for 16 or 19 h in the absence or presence of MG.

	Degeneration		Meiotic arrest		Meiotic progression		
	n	Deg.	*n*	GV	*n*	GVBD	PB
Control (16 h)	1019	12 (1.1%)	1007	50 (4.9%)	957	97 (10.6%)	860 (89.8%)
50-μM MG (16 h)	181	4 (2.2%)	177	16 (9.0%)	161	35 (21.7%)	126[a] (78.3%)
75-μM MG (16 h)	338	4 (1.2%)	334	11 (3.2%)	323	110 (28.6%)	213[a] (65.9%)
100-μM MG (16 h)	66	4[b] (6.1%)	62	4 (6.5%)	58	26 (44.8%)	32[a] (55.2%)
125-μM MG 16h	54	0 (0%)	54	13[a] (24%)	41	39[a] (92.7%)	2[a] (4.8%)
150-μM MG (16 h)	48	4 (8.3%)	44	0 (0%)	44	41[a] (93.1%)	3[a] (6.8%)
300-μM MG (16 h)	12	9[a] (75.0%)	3	0 (0%)	3	3 (100%)	0 (0%)
75-μM MG (19 h)	380	0 (0%)	380	24 (6.3%)	356	66 (18.5%)	290[c] (81.5%)

Significantly different from control; [a]$P < 0.001$; [b]$P < 0.01$. Significantly different from 16 h MG; [c]$P < 0.001$.

There was a significant arrest at GV stage (24%) in oocytes of MF-1 mice exposed to 125-μM MG during maturation for 16 h. Already 50-μM MG induced a significant meiosis I arrest (numbers with GVBD) and a significant reduction in PB oocytes compared with the control ($P < 0.001$; Table I). Rate of meiotic arrest at GVBD stage was even more increased to nearly 30% in the presence of 75-μM MG. For these reasons, we further used 75- or 100-μM MG to test for an influence of MG on spindle, chromosome segregation (see below), DNA integrity (in GV-arrested oocytes; see below) or mitochondrial distribution and redox state.

Unexpectedly, the rate of arrested GVBD oocytes dropped from 28.6 to 18.5%, when culture was prolonged from 16 to 19 h, and 81.5% of oocytes in the 75-μM MG group matured to MII during 19 h, not significantly different from the control cultured for 16 h. This suggests a meiotic delay by 75-μM MG.

Induction of DNA breaks in GV-stage oocytes

AGE may cause DNA breaks by induction of oxidative stress, ROS and DNA repair, or it may also cause apoptosis and cell death. Phosphorylated histone H2AX (γ-H2AX) is recruited to chromatin at sites of DNA repair in the oocyte nucleus, e.g. after vitrification (Trapphoff *et al.*, 2010). A low concentration of MG causes DNA damage in dictyate stage-arrested oocytes of the MF-1 mice since oocytes with over 20 foci (Fig. 4c″) significantly increased from 2.3 to 53.6% in the group exposed to 75-μM MG as compared with the control while those with 0–10 γ-H2AX-positive foci per nucleus (Fig. 4a″) decreased significantly from 77.6 to 22.6% (Supplementary data, Table SI).

Disturbances in spindle formation and chromosome congression

The analysis of spindle formation confirmed that progression through meiosis is significantly delayed by exposure of oocytes of MF-1 mice to 75-μM MG. After 16 h of maturation, the majority of the controls had progressed to MII (84.4%; Fig. 5a; Table II), while only 70.7% of the MG group possessed a polar body ($P < 0.05$). However, prolonged culture to 19 h resulted in an increase of oocytes with MII spindle to 93.5% (Fig. 5g and h). Control meiosis I-arrested oocytes possessed a normal bipolar spindle (5% were highly aberrant), while 69.5% of the MG group matured for 16 h possessed aberrant spindles as shown in Fig. 5b–d. Late anaphase I/telophase I stages were observed in this group (Fig. 5e and f), unlike in the controls progressing to meiosis II with well-aligned chromosomes and normal MII spindles (Fig. 5a). Some MG-exposed oocytes contained interphase-like chromatin within a nucleus-like state (Fig. 5f). The percentage of meiosis I oocytes in telophase I or with highly aberrant meiosis I spindle decreased to 28% by 19 h of culture when most oocytes were in meiosis II and had normal spindles (Fig. 5g and h), similar to the 16 h control (Fig. 5a; Table II). Unlike in the 16 h control, a large percentage of the MG-exposed meiosis I-arrested oocytes exhibited congression failure of chromosomes (69.5%) at 16 h of maturation (Fig. 5b–d) in contrast to controls (Fig. 5a; supplementary data, Table SII). Upon prolonged culture to 19 h, the percentage of oocytes in meiosis II with scattered chromosomes decreased to 6.9%, not significantly different from the control at 16 h (8%; Supplementary data, Table SII).

The failure in chromosome congression after 16 h maturation was associated with disturbances in spindle organization, in particular, with a failure to focus the acentriolar centrosomes recognized by pericentrin antibody at the spindle poles (Fig. 5b–d; supplementary data, Table SIII). Thus, pericentrin-reactive centrosomes were found either focused or more loosely assembled at the pole in 25 and 55%, respectively, of the meiosis I-arrested oocytes of the control, but in only 22.2 and 19.4% of the MG group at 16 h of culture. 53.2% of MG-exposed oocytes had displaced centrosomes away from the poles (e.g. Fig. 5c), but this decreased to 12.1% at 19 h, not different from controls (Supplementary data, Table SIII).

Delayed progression to anaphase I

In spite of possible increase in DNA breaks, the kinetics of GVBD was similar in living controls and oocytes exposed to 75-μM MG during *in vitro* maturation as analysed by polarizing microscopy (Fig. 6a).

When spindles were viewed non-invasively by the polarizing microscopy and time of anaphase I and telophase I progression and first polar body formation was quantitatively analysed (Fig. 6b and c), this confirmed that oocytes of the MG group progressed to

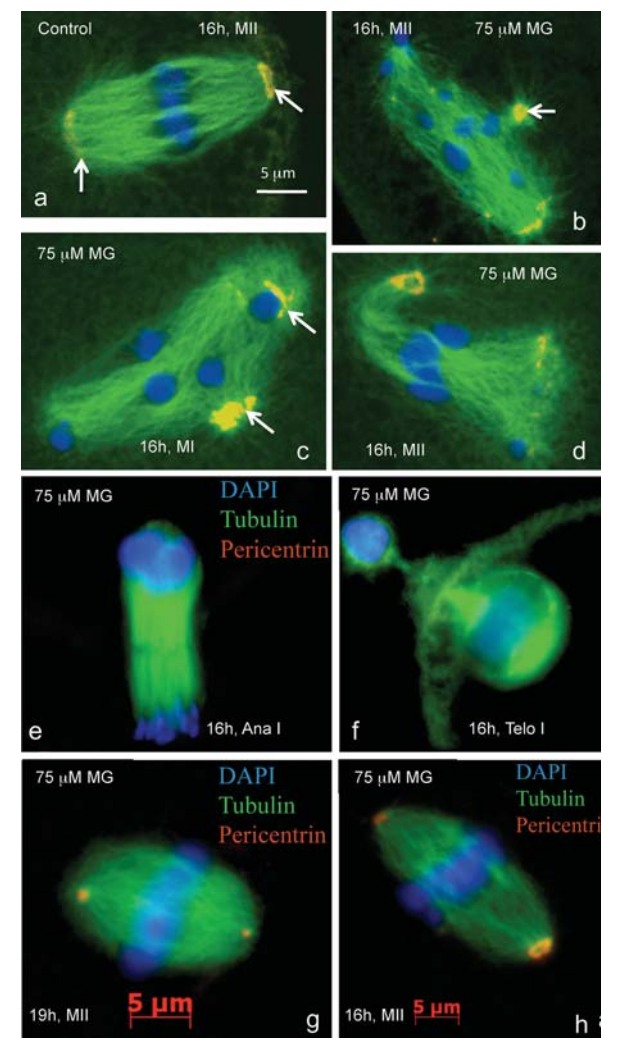

Figure 5 Spindles in control and oocytes of MF-1 mice exposed to 75-μM MG during maturation for 16 or 19 h. (**a**) Representative sample of control possessing a normal bipolar MII spindle (green), well-aligned chromosomes (blue) and pericentrin positive foci at centrosomes at the spindle poles (red, white arrows). (**b**) Bipolar spindle in MII oocyte with unaligned chromosomes and pericentrin at spindle pole as well as at one aster at spindle periphery (arrow). (**c**) Meiosis I oocyte with chromosome congression failure and unordered pericentrin foci at one pole, next to a chromosome (arrow) and at spindle periphery (white arrow) but not at the second spindle pole. (**d**) Aberrant tripolar spindle with some aligned chromosomes, one displaced chromosome close to an extra-pole, and two areas at poles with some pericentrin. (**e**) Delayed anaphase I spindle in oocyte matured for 16 h. (**f**) Delayed telophase I spindle with decondensed appearing chromatin after 16 h maturation in presence of MG. (**g**) Normal bipolar but relatively short spindle with one focus of pericentrin at each spindle pole and aligned chromosomes after 16 h of maturation in the presence of MG. (**h**) Fairly normal-appearing bipolar MII spindle with aligned chromosomes and normal pericentrin at poles in oocyte matured for 19 h in the presence of MG. Note, relative dense microtubules and intense tubulin staining close to centromeres in the part of the spindle and less intense staining for tubulin in the more peripheral spindle areas closer to the poles. White bar in (a) for (a–f) and red bars in (g) and (h): 5 μm.

anaphase I and emitted a polar body with a significant delay compared with the control (Fig. 6c).

Disturbances in chromosome condensation and anaphase I lagging

Delay in chromosome congression and anaphase I progression suggest that MG may critically affect attachment of chromosomes to the spindle and thereby induce a delayed release from the SAC. To test if this protects the oocytes from non-disjunction (for discussion see Vogt *et al.*, 2008, 2010), chromosomal constitution was analysed in oocytes matured in the presence of 75-μM MG for 16 or 19 h *in vitro* (Supplementary data, Figure S1; Table III). Only 66.4% of spread oocytes from the MG group compared with 88.9% in the control (Supplementary data, Figure S1a) possessed MII chromosomes (Dyads, Table III) after 16 h of culture ($P < 0.001$). The percentage increased to 77.8% in MG versus 88.3% in the control after 19 h of culture. Exclusively, oocytes in the MG group contained nucleus-like chromatin at 16 h and at 19 h of culture (Supplementary data, Figure S1, Table III). Aberrant chromosome condensation decreased to rates no more significantly different from control at 19 h of culture. At 16 h, anaphase I stages had profound lagging of chromosomes (Supplementary data, Figure S1), which was never observed in controls. However, the chromosomes in the MG group appeared more normal at 19 h of culture (Supplementary data, Figure S1d) suggesting an epigenetic effect in chromosome condensation by MG.

No MG-exposed oocyte contained an extra-chromosome and was hyperploid (aneuploidy; Table III). The increased number of oocytes containing less than 20 MII chromosomes (hypoploids) in the MG group spread at 16 h may relate to the still decondensed state of the chromosomes and likely represents a spreading artefact since hypoploidy was not much different between the MG group and controls when spreading was performed after 19 h of culture. Polyploidy rates and block in cytokinesis was not elevated in MG-exposed groups (Table III), and there was no evidence for precocious chromatid segregation.

Part C: Mitochondrial distribution and intra-mitochondrial redox state

Since it is suggested that MG affects mitochondrial function (Rabbani and Thornalley, 2008), and this could relate to alterations in spindle and chromosome condensation, we investigated mitochondrial distribution and inner membrane potential by JC-1 vital staining. Oocyte maturation for 7 h caused characteristically an accumulation of mitochondria with low-inner membrane potential (Ψ^{mit}) around the meiosis I spindle of control oocytes (Fig. 7a; supplementary data, Table SIV: group ++). A much larger percentage of oocytes exposed to 75 μM for 7 h compared with controls failed to assemble a prominent (++) or less dense but recognizable (+−) spindle-associated ring of mitochondria with low Ψ^{mit}. The majority of MG-treated oocytes exhibited a dispersed distribution of mitochondria (−−) (Fig. 8c; supplementary data, Table IV; $P < 0.05$). Oocyte maturation for 8 h in the presence of 100 μM MG did not cause significant changes. After 16 h of maturation, the majority of MII oocytes in the control and MG group exhibited a prominent spindle associated ring of low Ψ^{mit} mitochondria (Fig. 7d; 56.4 versus 70%, respectively; Supplementary data, Table IV). Therefore, efficient translocation of mitochondria towards the spindle appeared

Table II Meiotic spindle formation and spindle aberrations in MI or MII of denuded mouse oocytes of MF1 mice matured for 16 or 19 h in the absence or presence of 75 μM MG.

	Meiotic progression			MI spindle				MII spindle			
	n	MI (GVBD)	MII (PB)	*n*	Normal	Slightly aberrant	Totally aberrant	*n*	Normal	Slightly aberrant	Totally aberrant
Control	132	20 (15.5%)	112 (84.4%)	20	16 (80%)	3 (15%)	1 (5%)	112	82 (73.2%)	21 (18.75%)	9 (8%)
75-μM MG 16 h	157	46 (29.3%)	111[a] (70.7%)	46	10[b] (21.7%)	4 (8.7%)	32[c] (69.5%)	111	20 (18%)	22 (19.8%)	69[c] (62.1%)
75-μM MG 19 h	108	7 (6.5%)	101 (93.5%)	7	5 (71.5%)	0 (0%)	2 (28%)	101	76 (75.1%)	19 (14.2%)	6 (4.5%)

Significantly different from control; [a]$P < 0.05$; [b]$P < 0.01$; [c]$P < 0.001$.

delayed by MG. There was a significantly higher number of oocytes missing a cortical ring of mitochondria in the group matured for 8 h in the presence of 100-μM MG compared with controls (Fig. 7c; supplementary data, Table IV; $P < 0.05$), while there was no difference between treated and untreated groups at 16 h of maturation.

When Mito-Grx1-roGFP2 mRNA was injected into oocytes maintained in meiotic arrest for 8 h and then released to mature *in vitro* to MII (16 h) in the absence or presence of 100-μM MG, the fusion product was detected in mitochondria, e.g. those associated with the spindle (Fig. 8). After calibration of fully oxidized and reduced form of the Mito-Grx1-roGFP2 by treatment of oocytes with 10 mM H_2O_2 or 10 mM DTT (Fig. 8), the inner-mitochondrial GSH-dependent redox potential (E^m_{GSH}) was calculated in control and MG-exposed groups ($n = 32$ and $n = 21$ for control and MG groups, respectively) and shown to be significantly different: E^m_{GSH} was $-336{,}9$ mV with ± 2.1 mV standard error in the control group and -318.5 mV with ± 5.3 mV standard error in the MG group ($P < 0.005$). The distribution and GSH-dependent inner-mitochondrial potential was therefore disturbed by chronic, non-cytotoxic MG exposure.

Discussion

Different factors can influence sensitivity of mouse oocytes to MG-induced maturation arrest

Ageing may result in the accumulation of reactive carbonyl compounds leading to AGE formation in organs including the ovary (Tatone *et al.*, 2008; Tatone *et al.*, 2010). The semi-quantitative analysis of expression of GLO1 and GLO2 revealed for the first time that both of these enzymes are expressed in oocytes and cumulus cells and that the abundance of *Glo1* and *Glo2* mRNAs becomes dramatically reduced during oocyte maturation *in vivo*. While, oocytes can rely on an efficient detoxification of reactive carbonyl compounds spontaneously formed during normal cellular metabolism during GV stage, they become more sensitive to MG once resuming maturation. Proteome analysis suggests that GLO1 but not GLO2 is present in mouse MII oocytes (Wang *et al.*, 2010; Eichenlaub-Ritter, unpublished). Loss of transcripts for both glyoxalases following maturation is expected to weaken MG detoxification power, particularly after fertilization. The presence of an effective scavenging of reactive carbonyl compounds at GV stage suggests that oocytes are competent to deal with them mainly during their stay in

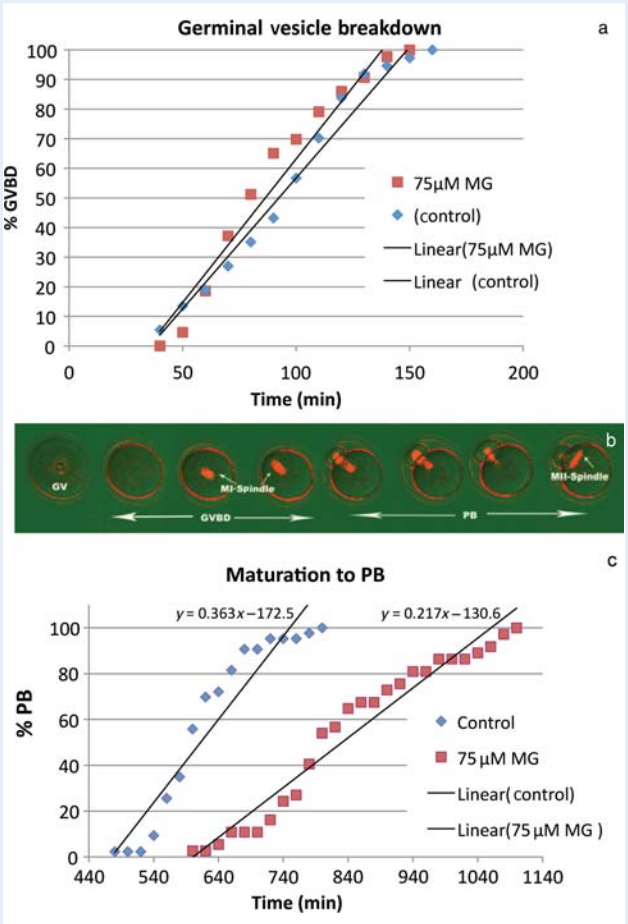

Figure 6 Non-invasive analysis of GVBD and PB formation of denuded oocytes from MF-1 mice by Octax polarization microscopy. (**a**) Kinetics of GVBD between 0 and 180 min maturation in the absence (control) or presence (75-μM MG) of MG is not significantly different between the two groups ($n = 37$ and 43, for control and MG groups, respectively). (**b**) Representative images of GV oocyte undergoing GVBD, forming a meiosis I spindle and progressing to anaphase I and telophase I with emitting the first PB and spindle formation at MII (white arrow). (**c**) Kinetics of PB formation differs significantly between control ($n = 43$ and 37 for control and MG groups, respectively; linear regression, $y = 0.363x - 172.5$) and MG group ($y = 0.217x - 130.6$; $P < 0.001$).

Table III Meiotic progression and chromosomal aberrations in oocytes of MF1 mice matured in the absence (control) or presence of MG for 16 or 19 h analysed for chromatin (restitution nucleus-like; aberrant chromosome condensation/sticky chromatin), aneuploidy or nuclear progression in the absence of cytokinesis (polyploidy).

	Meiotic progression			Restitution nucleus-like		Aberrant chromosome condensation		Aneuploidy			Polyploidy	
	n	Bivalents	Dyads	*n*	Meiosis I	*n*	Unusually condensed/sticky	*n*	Hypoploid (<20)	Euploid (20)	Hyperploid (>20)	*n*	Polypl. (40)
Control 16 h	152	17 (11.1%)	135 (88.9%)	152	0 (0%)	135	0 (0%)	93	3 (3.2%)	89 (95.6%)	1 (1.1%)	95	2 (3.5%)
75-μM MG 16 h	144	47 (32.6%)	97 (67.4%)	164	4 (2.4%)	97	18[c] (18.6%)	54	7 (13%)	47 (87%)	0 (0%)	57	3 (5.3%)
Control 19 h	112	13 (11.7%)	99 (88.3%)	97	0 (0%)	99	0 (0%)	71	0 (0%)	71 (100%)	0 (0%)	62	1 (1.6%)
75-μM MG 19 h	149	33 (22.2%)	116 (77.8%)	154	7 (4.5%)	116	3 (2.5%)	86	4 (4.7%)	82 (95.3%)	0 (0%)	87	1 (1.1%)

[a]$P < 0.001$; [b]$P < 0.05$; [c]$P < 0.001$.

the ovary. Although oocytes lack glycolytic enzymes and therefore may not produce substantial amounts of MG, they stimulate glycolysis of cumulus prior to and at maturation (Sugiura *et al.*, 2005; Su *et al.*, 2009). MG, which enters the oocyte initially through gap junctions, therefore poses a risk for induction of carbonyl stress, especially in the later stages of maturation and also in the embryo. MG concentration in cells is typically 2–4 μM; common test by chronic exposure use higher, median toxic concentrations around 300 μM–1 mM (Dobler *et al.*, 2006; Chan and Wu, 2008; Rabbani and Thornalley, 2010). During ageing, diabetes and PCOS when the ovary experiences carbonyl stress (Diamanti-Kandarakis *et al.*, 2007; Tatone *et al.*, 2008, 2010; Hsuuw *et al.*, 2005), oocytes may become chronically exposed to supra-physiological MG concentrations. Under these conditions, the presence in the oocyte of an efficient scavaging system is particularly relevant. Notably, the reduced rate of oocyte maturation in CEO but not DO from aged compared with young females indicates that cumulus of aged mice (and presumably other mammals like humans) has reduced capacity to protect oocytes from detrimental effects of MG, consistent with the view that chronological ageing affects expression of detoxifying enzymes (Di Loreto *et al.*, 2008). Increased MG as a metabolite from glycolysis might also contribute to adverse effects of high glucose on oocyte maturation in other conditions (Sutton-McDowall *et al.*, 2010). Since the cumulus is active in glycolysis during the comparatively long period of oocyte growth, the reduced protection can cause a continuous increase in formation of AGEs, a condition which we tried to mimic by exposing maturing oocytes to unphysiologically high concentrations of MG. In fact, this is shown to dramatically decrease and delay maturation, and affect spindle and chromosomes.

Since one-third of DO of young CD-1 females were still capable of maturing to MII in 300-μM MG, while there was already a significant meiotic arrest by 50-μM MG in oocytes of the MF-1 mice, and Chang and Chan (2010) reported reduced *in vitro* maturation in CEOs of hybrid ICR female mice by only 5-μM MG, genetic background, e.g. by differences in expression of detoxifying enzymes, may be important in response to carbonyl stress. It remains to be determined whether and in which way genetic background but also food consumption (e.g. with or without high phytohormones and radical scavengers), hormonal stimulation, culture conditions (e.g. presence of high or low O_2), or composition of culture media affect susceptibility of oocytes to MG, especially in the human. A recent study revealed that increased level of toxic AGEs in serum related to poor follicular and embryo development and reduced pregnancy rates, irrespective of maternal age (Jinno *et al.*, 2011), supporting the notion that carbonyl stress affects developmental potential of oocytes, including the human.

MG exposure affects DNA and chromatin condensation

Low concentrations of MG caused a significant rise in γ-H2AX spots in the GV of the meiotically arrested oocytes. H2AX histone characteristically undergoes phosphorylation at serine 139 in response to DNA damage and DNA double-strand breaks in somatic cells (e.g. Rogakou *et al.*, 1998; Tanaka *et al.*, 2006; Mah *et al.*, 2010). Knockout of the poly (ADP-ribose) polymerase (Parp-1) gene, which also causes persistence of γ-H2AX on the X chromosome bivalent in the mouse induces genome instability at oogenesis (Yang *et al.*, 2009). TUNEL-positive staining of nuclei in oocytes of the CD-1 mice as well

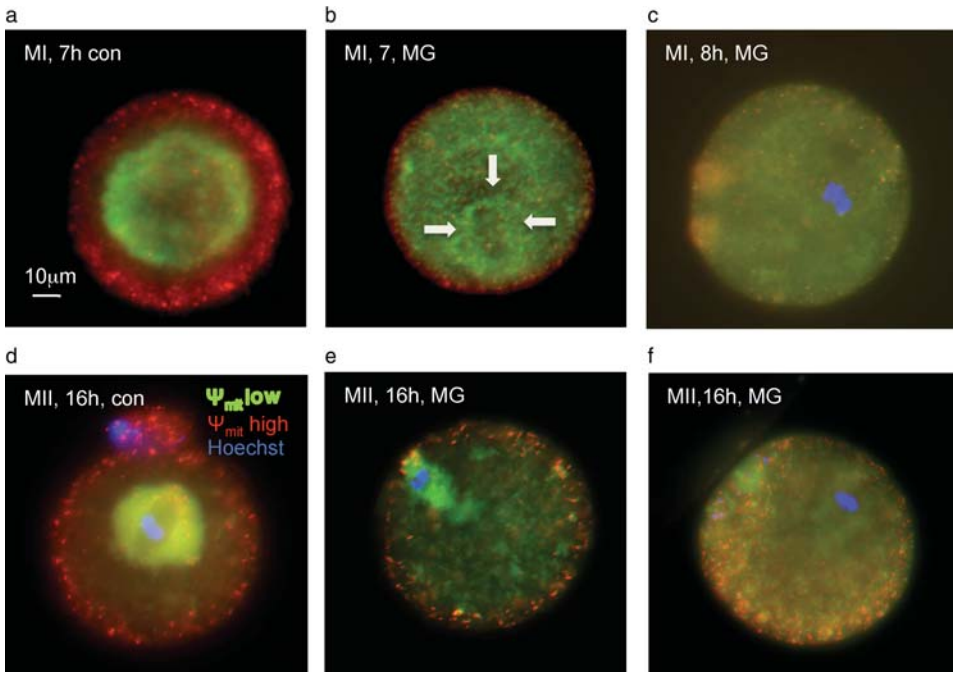

Figure 7 Distribution of JC-1 stained mitochondria in meiosis I (**a–c**) and meiosis II (**d–f**) oocytes of control (**a, d**) and MG-exposed groups (**b, c, e, f**). Representative samples of oocytes with prominent mitochondria aggregated around the spindle (**a, d**), with some association of mitochondria with spindle (**b**, arrows; **e**) and without accumulation around the spindle (**c, f**) are shown. Some cortical mitochondria with high potential of inner-mitochondrial membrane are visible in (**a, b, d, e**). See text for further explanation. Bar for (**a**–**f**) 10 μm.

disturbances in DNA integrity implicated by increased γ-H2AX by low MG (75 μM) in GV oocytes of MF-1 mice therefore support the notion that MG affects DNA integrity in resting as well as in maturing oocytes and such disturbances could contribute to reduced developmental potential.

In addition, the significant increase in oocytes with condensed, sticky chromatin, plus the presence of a restitution-like nucleus at meiosis I or meiosis II in spread and C-banded MG-exposed oocytes suggest an epigenetic effect of MG. Increases in ROS that are at the origin of adverse effects of MG (Chan *et al.*, 2005) may be particularly relevant and influence the fate of the oocyte after fertilization, e.g. such as an increased resorption of post-implantation embryos after *in vitro* fertilization of MG-exposed mouse oocytes and a decrease in fetal weight of the embryos, possibly as a result of increased apoptosis rate in the blastocyst (Chang and Chan, 2010). *In vivo* oocytes are presumably exposed to MG for prolonged periods, within the resting follicle but particularly also during follicular growth and development. Stochastic effects by MG and MG-induced carbonyl stress may therefore contribute to increases in DNA damage mimicked in our study by the comparatively short exposure of the GV-arrested oocyte to supra-physiological MG.

MG-effects on meiotic maturation, spindle formation, and chromosome congression

MG caused a dose-dependent meiotic arrest and delay at meiosis I at 16 h of maturation and a significant increase in oocytes with aberrant spindles, absence of polar centrosomal pericentrin and unaligned or lagging chromosomes, but there was no induction of aneuploidy. The delayed meiosis suggests that expression of the SAC inhibits oocytes with unattached chromosomes from progressing into anaphase I and in this way protects them from non-disjunction (Vogt *et al.*, 2008). Since there was no lagging-associated increase in non-disjunction in MG-exposed oocytes, activity of enzymes protecting from meiotic errors such as Aurora kinase B and mitotic centromere-associated kinesin (Vogt *et al.*, 2009, 2010; Illingworth *et al.*, 2010) appears also unaffected by MG. However, there is evidence that loss of chromosome cohesion and altered expression of products regulating centromere microtubule dynamics or SAC components occur with ageing (Pan *et al.*, 2008; Chiang *et al.*, 2010; Garcia-Cruz *et al.*, 2010; Lister *et al.*, 2010). Therefore, further work is required to assess the hypothesis that aged oocytes may have an increased susceptibility to MG-induced meiotic disturbances possibly acting synergistic to other aberrations (Eichenlaub-Ritter, 1998, 2003; Tatone *et al.*, 2008; Jones, 2008). To obtain more information on long-lasting effects of chronic, low MG-exposure, we are currently performing experiments with pre-antral follicle culture to further elucidate synergistic effects of chronic MG and increased carbonyl stress on the somatic as well as the oocyte compartment of the follicle.

Delayed distribution of mitochondria and altered inner-mitochondrial GSH-dependent redox potential

MG is well known to affect mitochondrial proteins and functions (Rabbani and Thornalley, 2010). MG concentration and carbonyl

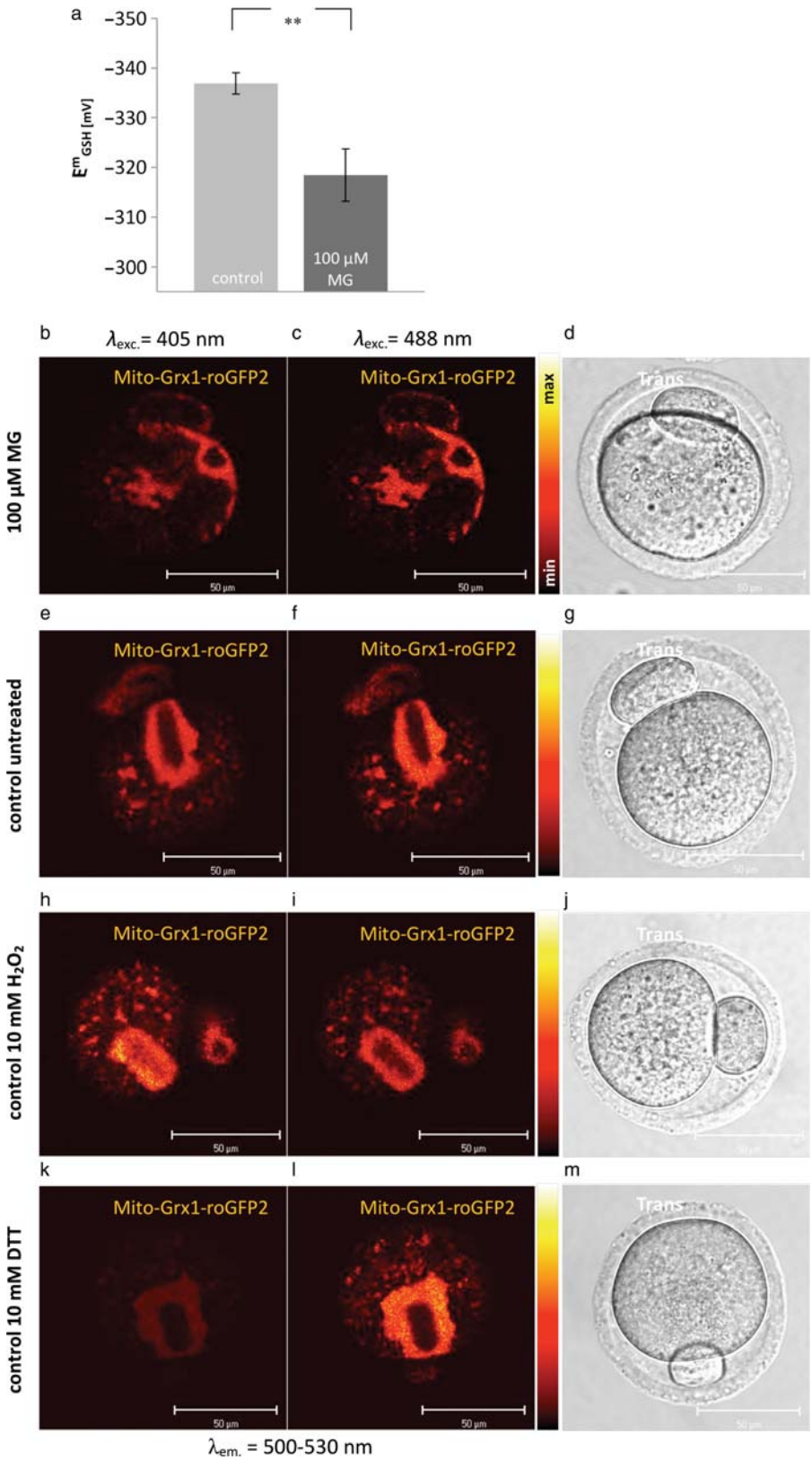

Figure 8 Oocytes expressing the mit-Grx1-roEGF2 fusion protein in mitochondria of oocytes: inner-mitochondrial GSH/GSSG redox potential in control (light grey bar) and MG-exposed MII oocytes (dark grey bar) (**a**) and representative images of MG-treated (**b**–**d**) and control MII oocytes (**e**–**g**) and controls exposed to 10 mM H_2O_2 (**h**–**j**) or 10 mM DTT (**k**–**m**) for calibration. See text for further explanation. Bar: 50 µm.

stress may not only be increased in aged ovary but also becomes increased under hyperglycaemic conditions. For instance, AGEs were increased in lean women with polycystic ovary syndrome (Diamanti-Kandarakis *et al*., 2008), and in serum from diabetic patients (Kilhovd *et al*., 2003; Lapolla *et al*., 2003). Interestingly, mitochondrial, dysfunction, and alterations in mitochondrial morphology and distribution, reduced ATP in pre-ovulatory and MII oocytes, and significant rises in abnormalities of the spindle and chromosome behaviour are characteristics of oocytes from a diabetic mouse model (Ratchford *et al*., 2007; Wang *et al*., 2010). Some of these effects could be mimicked by exposure of young and healthy, denuded mouse oocytes to MG such as spindle aberrations, concomitantly with delayed progression from proMI to MI (for discussion see Eichenlaub-Ritter *et al*., 2010a,b). The disturbance in mitochondrial accumulation might contribute or originate from disturbed spindle formation as an effect of altered ATP production (Yu *et al*., 2010). Since it is well known that calcium release and uptake are critically dependent on the activity of mitochondria after fertilization (recently reviewed by Dumollard *et al*., 2009; Swain and Pool, 2008; Van Blerkom, 2009), MG-caused mitochondrial dysfunction could also contribute to the reduced *in vitro* fertilization rate observed by Chang and Chan (2010) in MG-exposed CEO.

Expression of the RNA coding for the mitochondrial-targeted redox sensitive glutaredoxin1-roGPF2 fusion probe allowed us for the first time to determine the inner-mitochondrial GSH redox state in control and MG-exposed MII oocytes of a mammal. Mitochondria in oocytes are morphologically distinct and possess only few cristae (recently reviewed by Eichenlaub-Ritter *et al*., 2010a,b). However, their GSH redox potential in mitochondria was in a similar, only slightly lower range (around −340 mV) compared with what has been determined in cristae-rich mitochondria of HeLa cells (about −360 mV; Hanson *et al*., 2004). Maturation in the presence of MG significantly reduced the E^{m}_{GSH} in the MII oocytes, consistent with perturbation of regeneration of GSH by MG (Mannervik, 2008). GSH content within cytoplasm and mitochondria is in equilibrium and GSH presents the major buffer against oxidative stress in oocytes (for discussion see Eichenlaub-Ritter *et al*., 2010a,b). The reduced E^{m}_{GSH} in mouse oocytes exposed to MG reflects therefore disturbed redox regulation and may be responsible for the dose-dependently reduced and delayed oocyte maturation rate. Similarly, this may contribute to reduced oocyte quality in mice exposed to low MG in drinking water with lower maturation, fertilization and *in vivo* development rates of embryos compared with controls (Chang and Chan (2010). Further studies have to show whether substitution of culture medium with GSH donor (Curnow *et al*., 2010) might reduce some of the MG adverse effects on oocytes.

In conclusion, the disturbances in redox regulation and distribution of mitochondria by MG as well as epigenetic effects on chromatin may be responsible for aberrant and delayed spindle formation. In aged oocytes with reduced defence and protection by cumulus cells as well as altered expression patterns and chromosome cohesion in oocytes, MG exposure may therefore contribute to predisposion to aneuploidy, although it did not induce aneuploidy in the 'young' model. In addition, disturbed redox regulation, cell cycle progression and epigenetic effects by exposure to MG are critical for fertilization and early embryogenesis in mammals and may contribute to reduced oocyte quality and developmental potential, e.g. in oocytes of aged females or such coming from patients suffering from metabolic disease like diabetes and containing high toxic AGEs in serum (Jinno *et al*., 2011), follicular fluid and follicle.

Supplementary data

Supplementary data are available at http://humrep.oxfordjournals.org/.

Authors' roles

C.T. and U.E.-R. took part in study design, supervision, coordination and drafting of manuscript. C.T., T.H., G.D.E., P.T. and F.A. took part in study execution, and data collection and discussion. T.S. took part in study design, supervision and data analysis of redox regulation, drafting of manuscript.

Acknowledgements

We thank Ilse Betzendahl for expert technical assistance. We gratefully acknowledge the gift of the probe for the mito-Grx1-roGFP2 from Andreas Meyer (Tübingen). We thank Rudolf Eichenlaub for critical reading of the manuscript.

Funding

The work has been supported by the German Research Foundation (DFG) (FOR1041) (U.E.), the Ministero dell'Università e della Ricerca Scientifica (C.T.) and University of L'Aquila and Regione Abruzzo (RE.C.O.TE.S.S.C.-POR 2007-2013) (G.D.).

References

Amicarelli F, Colafarina S, Cattani F, Cimini A, Di Ilio C, Ceru MP, Miranda M. Scavenging system efficiency is crucial for cell resistance to ROS-mediated methylglyoxal injury. *Free Radic Biol Med* 2003; **35**:856–871.

Baynes JW. The role of AGEs in aging: causation or correlation. *Exp Gerontol* 2001;**36**:1527–1537.

Bradshaw J, Jung T, Fulka J Jr., Moor RM. UV irradiation of chromosomal DNA and its effect upon MPF and meiosis in mammalian oocytes. *Mol Reprod Dev* 1995;**41**:503–512.

Broekmans FJ, Soules MR, Fauser BC. Ovarian aging: mechanisms and clinical consequences. *Endocr Rev* 2009;**30**:465–493.

Chan WH, Wu HJ. Methylglyoxal and high glucose co-treatment induces apoptosis or necrosis in human umbilical vein endothelial cells. *J Biol Chem* 2008;**103**:1144–1157.

Chan WH, Wu HJ, Hsuuw YD. Curcumin inhibits ROS formation and apoptosis in methylglyoxal-treated human hepatoma G2 cells. *Ann N Y Acad Sci* 2005;**1042**:372–378.

Chang YJ, Chan WH. Methylglyoxal has injurious effects on maturation of mouse oocytes, fertilization, and fetal development, via apoptosis. *Toxicol Lett* 2010;**193**:217–223.

Chiang T, Duncan FE, Schindler K, Schultz RM, Lampson MA. Evidence that weakened centromere cohesion is a leading cause of age-related aneuploidy in oocytes. *Curr Biol* 2010;**20**:1522–1528.

Cukurcam S, Hegele-Hartung C, Eichenlaub-Ritter U. Meiosis-activating sterol protects oocytes from precocious chromosome segregation. *Hum Reprod* 2003;**18**:1908–1917.

Cukurcam S, Betzendahl I, Michel G, Vogt E, Hegele-Hartung C, Lindenthal B, Eichenlaub-Ritter U. Influence of follicular fluid meiosis-activating sterol on aneuploidy rate and precocious chromatid segregation in aged mouse oocytes. *Hum Reprod* 2007;**22**:815–828.

Curnow EC, Ryan JP, Saunders DM, Hayes ES. In vitro developmental potential of macaque oocytes, derived from unstimulated ovaries, following maturation in the presence of glutathione ethyl ester. *Hum Reprod* 2010;**25**:2465–2474.

Di Loreto S, Zimmitti V, Sebastiani P, Cervelli C, Falone S, Amicarelli F. Methylglyoxal causes strong weakening of detoxifying capacity and apoptotic cell death in rat hippocampal neurons. *Int J Biochem Cell Biol* 2008;**40**:245–257.

Diamanti-Kandarakis E, Piperi C, Korkolopoulou P, Kandaraki E, Levidou G, Papalois A, Patsouris E, Papavassiliou AG. Accumulation of dietary glycotoxins in the reproductive system of normal female rats. *J Mol Med* 2007;**85**:1413–1420.

Diamanti-Kandarakis E, Baillargeon JP, Nestler JE, Ostlund RE, Teimuraz Apridonidze. Greek hyperinsulinemic women, with or without polycystic ovary syndrome, display altered inositols metabolism. *Hum Reprod* 2008;**23**:1439–1446.

Dobler D, Ahmed N, Song L, Eboigbodin KE, Thornalley PJ. Increased dicarbonyl metabolism in endothelial cells in hyperglycemia induces anoikis and impairs angiogenesis by RGD and GFOGER motif modification. *Diabetes* 2006;**55**:1961–1969.

Dumollard R, Carroll J, Duchen MR, Campbell K, Swann K. Mitochondrial function and redox state in mammalian embryos. *Semin Cell Dev Biol* 2009;**20**:346–353.

Eichenlaub-Ritter U. Genetics of oocyte ageing. *Maturitas* 1998; **30**:143–169.

Eichenlaub-Ritter U. Aneuploidy in ageing oocytes and after toxic insult. In Traonson AO, Gosden RG (eds). *Biology and Pathology of the Oocyte*. Cambridge, UK: Cambridge University Press, 2003,220–257.

Eichenlaub-Ritter U, Betzendahl I. Chloral hydrate induced spindle aberrations, metaphase I arrest and aneuploidy in mouse oocytes. *Mutagenesis* 1995;**10**:477–486.

Eichenlaub-Ritter U, Boll I. Nocodazole sensitivity, age-related aneuploidy, and alterations in the cell cycle during maturation of mouse oocytes. *Cytogenet Cell Genet* 1989;**52**:170–176.

Eichenlaub-Ritter U, Vogt E, Yin H, Gosden R. Spindles, mitochondria and redox potential in ageing oocytes. *Reprod Biomed Online* 2004;**8**:45–58.

Eichenlaub-Ritter U, Staubach N, Trapphoff T. Chromosomal and cytoplasmic context determines predisposition to maternal age-related aneuploidy: brief overview and update on MCAK in mammalian oocytes. *Biochem Soc Transac* 38, Part 6 2010a.

Eichenlaub-Ritter U, Wieczorek M, Seidel T. Age related changes in mitochondrial function and new approaches to study redox regulation in mammalian oocytes in response to age or maturation conditions. *Mitochondrion* 2010b (doi:10.1016/j.mito.2010.08.011).

Fujii EY, Nakayama M. The measurements of RAGE, VEGF, and AGEs in the plasma and follicular fluid of reproductive women: the influence of aging. *Fertil Steril* 2010;**94**:694–700.

Garcia-Cruz R, Brieño MA, Roig I, Grossmann M, Velilla E, Pujol A, Cabero L, Pessarrodona A, Barbero JL, Caldés MG. Dynamics of cohesin proteins REC8, STAG3, SMC1 beta and SMC3 are consistent with a role in sister chromatid cohesion during meiosis in human oocytes. *Hum Reprod* 2010;**25**:2316–2327.

Grøndahl ML, Yding Andersen C, Bogstad J, Nielsen FC, Meinertz H, Borup R. Gene expression profiles of single human mature oocytes in relation to age. *Hum Reprod* 2010;**25**:957–968.

Gutscher M, Pauleau AL, Marty L, Brach T, Wabnitz GH, Samstag Y, Meyer AJ, Dick TP. Real-time imaging of the intracellular glutathione redox potential. *Nat Methods* 2008;**5**:553–559.

Hamatani T, Falco G, Carter MG, Akutsu H, Stagg CA, Sharov AA, Dudekula DB, VanBuren V, Minoru SHKo. Age-associated alteration of gene expression patterns in mouse oocytes. *Hum Mol Gen* 2004; **13**:2263–2278.

Hanson GT, Aggeler R, Oglesbee D, Cannon M, Capaldi RA, Tsien RY, Remington SJ. Investigating mitochondrial redox potential with redox-sensitive green fluorescent protein indicators. *J Biol Chem* 2004; **279**:13044–13053.

Harman D. Free radical theory of aging: an update: increasing the functional life span. *Ann N Y Acad Sci* 2006;**1067**:10–21.

Hassold T, Hunt P. Maternal age and chromosomally abnormal pregnancies: what we know and what we wish we knew. *Curr Opin Pediatr* 2009;**21**:703–708.

Holt JE, Jones KT. Control of homologous chromosome division in the mammalian oocyte. *Mol Hum Reprod* 2009;**15**:139–147.

Hsuuw YD, Chang CK, Chan WH, Yu JS. Curcumin prevents methylglyoxal-induced oxidative stress and apoptosis in mouse embryonic stem cells and blastocysts. *J Cell Physiol* 2005;**205**:379–386.

Illingworth C, Pirmadjid N, Serhal P, Howe K, Fitzharris G. MCAK regulates chromosome alignment but is not necessary for preventing aneuploidy in mouse oocyte meiosis I. *Development* 2010;**137**:2133–2138.

Jinno M, Takeuchi M, Watanabe A, Teruya K, Hirohama J, Eguchi N, Miyazaki A. Advanced glycation end-products accumulation compromises embryonic development and achievement of pregnancy by assisted reproductive technology. *Hum Reprod* 2011;**26**:604–610.

Jones KT. Meiosis in oocytes: predisposition to aneuploidy and its increased incidence with age. *Hum Reprod Update* 2008;**14**:143–158.

Kilhovd BK, Giardino I, Torjesen PA, Birkeland KI, Berg TJ, Thornalley PJ, Brownlee M, Hanssen KF. Increased serum levels of the specific AGE-compound methylglyoxal-derived hydroimidazolone in patients with type 2 diabetes. *Metabolism* 2003;**52**:163–167.

Kuhla B, Lüth HJ, Haferburg D, Weick M, Reichenbach A, Arendt T, Münch G. Pathological effects of glyoxalase I inhibition in SH-SY5Y neuroblastoma cells. *J Neurosci Res* 2006;**83**:1591–1600.

Lapolla A, Flamini R, Dalla Vedova A, Senesi A, Reitano R, Fedele D, Basso E, Seraglia R, Traldi P. Glyoxal and methylglyoxal levels in diabetic patients: quantitative determination by a new GC/MS method. *Clin Chem Lab Med* 2003;**41**:1166–1173.

Ledl F, Schleicher E. The Maillard reaction in food and in human body, new results in chemistry, biochemistry and medicine. *Angew Chem Int Ed Engl* 1999;**29**:565–706.

Lister LM, Kouznetsova A, Hyslop LA, Kalleas D, Pace SL, Barel JC, Nathan A, Floros V, Adelfalk C, Watanabe Y *et al.*. Age-Related meiotic segregation errors in mammalian oocytes are preceded by depletion of cohesin and Sgo2. *Curr Biol* 2010;**20**:1511–1521.

Llopis J, McCaffery JM, Miyawaki A, Farquhar MG, Tsien RY. Measurement of cytosolic, mitochondrial, and Golgi pH in single living cells with green fluorescent proteins. *Proc Natl Acad Sci USA* 1998;**95**:6803–6808.

Lopes FL, Fortier AL, Darricarrère N, Chan D, Arnold DR, Trasler JM. Reproductive and epigenetic outcomes associated with aging mouse oocytes. *Hum Mol Genet* 2009;**18**:2032–2044.

Mah LJ, El-Osta A, Karagiannis TC. GammaH2AX: a sensitive molecular marker of DNA damage and repair. *Leukemia* 2010;**24**:679–686.

Mannervik B. Molecular enzymology of the glyoxalase system. *Drug Metabol Drug Interact* 2008;**23**:13–27.

Meyer AJ, Dick TP. Fluorescent protein-based redox probes. *Antioxid Redox Signal* 2010;**13**:621–650.

Morcos M, Du X, Pfisterer F, Hutter H, Sayed AA, Thornalley P, Ahmed N, Baynes J, Thorpe S, Kukudov G *et al.* Glyoxalase-1 prevents mitochondrial protein modification and enhances lifespan in Caenorhabditis elegans. *Aging Cell* 2008;**7**:260–269.

Nogueira D, Cortvrindt R, Everaerdt B, Smitz J. Effects of long-term in vitro exposure to phosphodiesterase type-3 inhibitors on follicle and oocyte development. *Reproduction* 2005;**130**:177–186.

Pan H, Ma P, Zhu W, Schultz RM. Age-associated increase in aneuploidy and changes in gene expression in mouse eggs. *Dev Biol* 2008; **316**:397–407.

Quinn P, Barros C, Whittingham DG. Preservation of hamster oocytes to assay the fertilizing capacity of human spermatozoa. *J Reprod Fertil* 1982; **66**:161–168.

Rabbani N, Thornalley PJ. Dicarbonyls linked to damage in the powerhouse: glycation of mitochondrial proteins and oxidative stress. *Biochem Soc Trans* 2008;**36**:1045–1050.

Rabbani N, Thornalley PJ. Methylglyoxal, glyoxalase I and the dicarbonyl proteome. *Amino Acids* 2010. doi:10.1007/s00726–010-0783-0 (in press).

Ratchford AM, Chang AS, Chi MM, Sheridan R, Moley KH. Maternal diabetes adversely affects AMP-activated protein kinase activity and cellular metabolism in murine oocytes. *Am J Physiol Endocrinol Metab* 2007;**293**:1198–1206.

Rattan SI. Increased molecular damage and heterogeneity as the basis of aging. *Biol Chem* 2008;**389**:267–272.

Roberts R, Iatropoulou A, Ciantar D, Stark J, Becker DL, Franks S, Hardy K. Follicle-stimulating hormone affects metaphase I chromosome alignment and increases aneuploidy in mouse oocytes matured in vitro. *Biol Reprod* 2005;**72**:107–118.

Rogakou EP, Pilch DR, Orr AH, Ivanova VS, Bonner WM. DNA double-stranded breaks induce histone H2AX phosphorylation on serine 139. *J Biol Chem* 1998;**273**:5858–5868.

Schafer FQ, Buettner GR. Redox environment of the cell as viewed through the redox state of the glutathione disulfide/glutathione couple. *Free Radic Biol Med* 2001;**30**:1191–1212.

Schmidt AM, Yan SD, Yan SF, Stern DM. The biology of the receptor for advanced glycation end products and its ligands. *Biochim Biophys Acta* 2000;**1498**:99–111.

Shen Y, Betzendahl I, Tinneberg HR, Eichenlaub-Ritter U. Enhanced polarizing microscopy as a new tool in aneuploidy research in oocytes. *Mutat Res* 2008;**651**:131–140.

Shinohara M, Thornalley PJ, Giardino I, Beisswenger P, Thorpe S, Onorato J, Brownlee M. Overexpression of glyoxalase-I in bovine endothelial cells inhibits intracellular advanced glycation endproduct formation and prevents hyperglycemia-induced increases in macromolecular endocytosis. *J. Clin Invest* 1998;**101**:1142–1147.

Steuerwald NM, Bermúdez MG, Wells D, Munné S, Cohen J. Maternal age-related differential global expression profiles observed in human oocytes. *Reprod Biomed Online* 2007;**14**:700–708.

Su YQ, Sugiura K, Eppig JJ. Mouse oocyte control of granulosa cell development and function: paracrine regulation of cumulus cell metabolism. *Semin Reprod Med* 2009;**27**:32–42.

Sugiura K, Pendola FL, Eppig JJ. Oocyte control of metabolic cooperativity between oocytes and companion granulosa cells: energy metabolism. *Dev Biol* 2005;**279**:20–30.

Sun F, Betzendahl I, Shen Y, Cortvrindt R, Smitz J, Eichenlaub-Ritter U. Preantral follicle culture as a novel in vitro assay in reproductive toxicology testing in mammalian oocytes. *Mutagenesis* 2004;**19**:13–25.

Sutton-McDowall ML, Gilchrist RB, Thompson JG. The pivotal role of glucose metabolism in determining oocyte developmental competence. *Reproduction* 2010;**139**:685–695.

Swain JE, Pool TB. ART failure: oocyte contributions to unsuccessful fertilization. *Hum Reprod Update* 2008;**14**:431–446.

Tanaka T, Kurose A, Huang X, Traganos F, Dai W, Darzynkiewicz Z. Extent of constitutive histone H2AX phosphorylation on *Ser*-139 varies in cells with different TP53 status. *Cell Prolif* 2006;**39**:313–323.

Tatone C, Carbone MC, Gallo R, Delle Monache S, Di Cola M, Alesse E, Amicarelli F. Age-associated changes in mouse oocytes during postovulatory in vitro culture: possible role for meiotic kinases and survival factor BCL2. *Biol Reprod* 2006;**74**:395–402.

Tatone C, Amicarelli F, Carbone MC, Monteleone P, Caserta D, Marci R, Artini PG, Piomboni P, Focarelli R. Cellular and molecular aspects of ovarian follicle ageing. *Hum Reprod Update* 2008;**14**:131–142.

Tatone C, Carbone MC, Campanella G, Festuccia C, Artini PG, Talesa V, Focarelli R, Amicarelli F. Female reproductive dysfunction during ageing: role of methylglyoxal in the formation of advanced glycation endproducts in ovaries of reproductively-aged mice. *J Biol Regul Homeost Agents* 2010;**24**:63–72.

Thornalley PJ. Protecting the genome: defence against nucleotide glycation and emerging role of glyoxalase I overexpression in multidrug resistance in cancer chemotherapy. *Biochem Soc Trans* 2003;**31**:1372–1377.

Thornalley PJ, McLellan AC, Lo TW, Benn J, Sonksen PH. Negative association between erythrocyte reduced glutathione concentration and diabetic complications. *Clin Sci* 1996;**91**:575–582.

Thouas GA, Trounson AO, Jones GM. Effect of female age on mouse oocyte developmental competence following mitochondrial injury. *Biol Reprod* 2005;**73**:366–373.

Trapphoff T, El Hajj N, Zechner U, Haaf T, Eichenlaub-Ritter U. DNA integrity, growth pattern, spindle formation, chromosomal constitution and imprinting patterns of mouse oocytes from vitrified preantral follicles. *Hum Reprod* 2010. doi: 10.1093/humrep/deq278.

Van Blerkom J. Mitochondria in early mammalian development. *Semin Cell Dev Biol* 2009;**20**:354–364.

Van Blerkom J, Sinclair J, Davis P. Mitochondrial transfer between oocytes: potential applications of mitochondrial donation and the issue of heteroplasmy. *Hum Reprod* 1998;**13**:2857–2868.

Van Blerkom J, Davis P, Mathwig V, Alexander S. Domains of high-polarized and low-polarized mitochondria may occur in mouse and human oocytes and early embryos. *Hum Reprod* 2002;**17**:393–406.

Van Blerkom J, Davis P, Thalhammer V. Regulation of mitochondrial polarity in mouse and human oocytes: the influence of cumulus derived nitric oxide. *Mol Hum Reprod* 2008;**14**:431–444.

Verzijl N, Degroot J, Oldehinkel E, Bank RA, Thorpe SR, Baynes JW, Bayliss MT, Bijlsma JWJ, Lafeber F, Tekoppele JM. Age-related accumulation of Maillard reaction products in human articular cartilage collagen. *Biochem J* 2000;**350**:381–387.

Vogt E, Eichenlaub-Ritter U, Winterscheid U, Shen Y, Tinneberg HR, Sorensen R. 2-Methoxyestradiol induces spindle aberrations, chromosome congression failure, and nondisjunction in mouse oocytes. *Biol Reprod* 2007;**76**:784–793.

Vogt E, Kirsch-Volders M, Parry J, Eichenlaub-Ritter U. Spindle formation, chromosome segregation and the spindle checkpoint in mammalian oocytes and susceptibility to meiotic error. *Mutat Res* 2008;**651**:14–29.

Vogt E, Kipp A, Eichenlaub-Ritter U. Aurora kinase B, epigenetic state of centromeric heterochromatin and chiasma resolution in oocytes. *Reprod Biomed Online* 2009;**19**:352–368.

Vogt E, Sanhaji M, Klein W, Seidel T, Wordeman L, Eichenlaub-Ritter U. MCAK is present at centromeres, midspindle and chiasmata and involved in silencing of the spindle assembly checkpoint in mammalian oocytes. *Mol Hum Reprod* 2010;**16**:665–684.

Wang YC, Tsai YS, Huang JL, Lee KW, Kuo CC, Wang CS, Huang AM, Chang JY, Jong YJ, Lin CS. Arecoline arrests cells at prometaphase by deregulating mitotic spindle assembly and spindle assembly checkpoint: implication for carcinogenesis. *Oral Oncology* 2010;**46**:255–262.

Wautier MP, Chappey O, Corda S, Stern DM, Schmidt AM, Wautier JL. Activation of NADPH oxidase by AGE links oxidant stress to altered gene expression via RAGE. *Am J Physiol Endocrinol Metab* 2001; **280**:E685–E694.

Yang F, Baumann C, De La Fuente R. Persistence of histone H2AX phosphorylation after meiotic chromosome synapsis and abnormal centromere cohesion in poly (ADP-ribose) polymerase (Parp-1) null oocytes. *Dev Biol* 2009;**331**:326–338.

Yin D, Chen K. The essential mechanisms of aging: irreparable damage accumulation of biochemical side-reactions. *Exp Gerontol* 2005; **40**:455–465.

Yin L, Morita A, Tsuji T. Skin aging induced by ultraviolet exposure and tobacco smoking: evidence from epidemiological and molecular studies. *Photoderm Photoim Photomed* 2001;**17**:178–183.

Yu Y, Dumollard R, Rossbach A, Lai FA, Swann K. Redistribution of mitochondria leads to bursts of ATP production during spontaneous mouse oocyte maturation. *J Cell Physiol* 2010; **224**:672–680.